High-Performance Self-Compacting Concrete with Recycled Aggregates from the Precast Industry: Durability Assessment

Tiago Barroqueiro [1], Pedro R. da Silva [2] and Jorge de Brito [3,*]

[1] Civil Engineering Master, Instituto Superior Técnico, Universidade de Lisboa, 1049-001 Lisbon, Portugal; tiagobarroqueiro87@gmail.com

[2] CERIS, Instituto Superior de Engenharia de Lisboa, Instituto Politécnico de Lisboa, 1959-007 Lisboa, Portugal; silvapm@dec.isel.pt

[3] CERIS, Instituto Superior Técnico, Universidade de Lisboa, 1049-001 Lisbon, Portugal

*   Correspondence: jb@civil.ist.utl.pt

Abstract: The main objective of this paper is to provide the industry with a simple and practical way of disposing and recovering recycled waste from precast reinforced concrete elements rejected during the quality control process, while minimizing the consumption of natural resources in the production of concrete and, consequently, significantly reducing the environmental impact of both (construction and demolition waste and extracting natural aggregates). In other words, with this work, the intention is to evaluate the feasibility of producing high-performance self-compacting concrete with a less environmental impact, by replacing natural aggregates (NA) with fine and coarse recycled aggregates resulting from the precast industry, which allows the future use of this type of aggregates in the industrial process without reservations concerning the expected durability performance. To achieve these objectives, six types of self-compacting concrete (SCC) were produced incorporating different amounts of recycled aggregates. Six replacement ratios for fine recycled aggregates (FRA) and coarse recycled aggregates (CRA) were considered: (FRA/CRA) 0/0; 25/25; 50/50; 100/100; 0/100 and 100/0%. Six different tests were carried out to characterize both the main concrete transport mechanisms and the main concrete degradation mechanisms, namely: the immersion water absorption test, capillary water absorption test, oxygen permeability test, chloride migration test, electrical resistivity test and carbonation test. The obtained results clearly demonstrate that, despite the negative influence of the inclusion of recycled aggregates, it is still possible to produce high-performance self-compacting concrete with perfectly acceptable durability properties.

Keywords: self-compacting concrete; coarse and fine recycled aggregates from the precast industry; durability properties

1. Introduction

Since the beginning of the industrial revolution, the concentration of CO_2 in the atmosphere has increased from 280 to 400 ppm in 2014 [1]. According to experts, to avoid climate change in the second half of the 21st century, CO_2 emissions must be reduced by 90% by 2030 [2]. Today, the annual production of concrete is approximately 1×10^{10} tonnes. This results in large amounts of CO_2 emissions due, essentially, to the natural aggregates (NA) extraction and to the production of Portland cement. It is estimated that 1.7–2.1 tonnes of natural resources are used as raw material per m^3 of concrete produced [3]. Given this current state, there is an urgent need to change the methods and principles of concrete manufacturing processes and to evaluate in detail the use of various residues in the concrete production. The use of some recycled materials, such as recycled aggregates (RA), can prevent the

consumption of natural resources, save energy, reduce the concrete cost production and be very beneficial for the environment due to the reduction of air pollution, among other environmental impacts [4].

In order to respond to the concrete durability problems, as well as search for improving its behavior in aggressive environments, new types of concrete have emerged associated with new technologies. This is the case of self-compacting concrete (SCC), which arises initially to respond to durability problems associated with the lack of specialized labor, but which has numerous other advantages such as the reduction of noise associated with vibration, shorter execution times and more perfect finishing surfaces, among others [5]. The fresh-state SCC properties are the main difference to a conventional concrete (CC), although they may have the same mechanical properties in the hardened state. However, and due to the differences presented between them regarding the mix proportions and the placement process, the SCC durability may be different from that presented by a CC, requiring this aspect further investigation. In this sense, a lot of work has been done in the study of SCC in its fresh and hardened state, in the methods of calculating its mix proportions and in the processes of casting on site. However, only a few works have addressed the verification and optimization of SCC in terms of durability, particularly using high-performance mixes with incorporation of recycled aggregates (RA) from the precast industry. It is even common to find contradictory results regarding the different transport mechanisms (permeability, diffusion and capillarity) [5].

Regarding the use of precast concrete elements by the construction industry, the incentives from some organizations, mainly Europeans, for its increase as a means of optimizing resources in production and of a higher performance of reinforced concrete structures should be highlighted. For example, the British Precast Concrete Federation [6] has since 2013 encouraged concrete precast companies to increase the sustainability of the elements produced as well as the production methods used. There is a significant increase in the production of precast concrete elements throughout Europe with a special focus on, for example, the Netherlands, where it already represents approximately 45% of the construction solutions, or Germany, where this value corresponds to approximately 38% [7]. It is also worth mentioning that significant amounts of precast concrete elements are rejected due to flaws in the manufacturing process leading to characteristics incompatible with the quality and performance requirements prescribed in the specifications. All of this implies, on the one hand, the interest in producing increasingly more concrete elements with a high-performance and, on the other hand, a significant amount of good quality concrete waste with high processing costs. Therefore, the possibility and interest in producing a high-performance self-compacting concrete (HPSCC) comes up, incorporating these RA as a way to solve the various problems mentioned.

There are already some scattered studies on some of the problems presented, and the following should be highlighted: Ozbakkaloglu et al. [8] evaluated the water absorption of concrete with replacement ratios of NA for RA of 25%, 50% and 100% and reported an increase in this absorption with the increase in the replacement ratio. The authors also state that, for replacement ratios of 100%, the losses in durability are significant. Dimitriou et al. [9] also refer performance losses of the main transport mechanisms with the increase in the replacement ratio of NA for RA (replaced at 50–100%). The authors identify as the main cause for the obtained results the quantity and quality of the mortar adhered to the surface of the RA. With results similar to those mentioned, Alexandridou et al. [10] emphasize the performance loss of concrete with NA to RA replacement ratios of 0%, 25% and 75%.

On the other hand, Poon et al. [11,12] report significantly more promising results for high-performance concrete produced with coarse recycled aggregates (CRA). The authors state that the microstructural properties of the aggregate/binder transition zone are one of the main causes for possible performance loss of these concrete mixes. Likewise, other authors have promising results in concrete with CRA for replacement ratios of up to 100%. Tam et al. [13] refer, for example, that through simple changes in the mixing process it is possible to obtain significant improvements in the microstructure of the aggregate/binder transition zone with relevant improvement of the overall concrete durability.

Regarding the use of fine recycled aggregates (FRA), it is possible to mention less favorable results when compared with the use of CRA. In this sense, Evangelista and de Brito [14] highlight the viability of concrete production with FRA with positive results for FNA replacement ratios of up to 30%. Analogously, Thomas et al. [15] emphasize more conservative values for the use of FRA replacing FNA with maximum permissible replacement ratios in the order of 20%.

In the particular case of RA from precast concrete elements, there are still few works carried out. Nevertheless, Soares et al. [16] present work on the use of CRA from precast rejects concrete elements where they highlight the quality of these aggregates as well as their influence on improving the performance of the produced concrete when compared with conventional RA. Similarly, other authors refer analogous consequences regarding the quality of these aggregates from precast elements [17–20].

In this context, the main objective of the present work is to evaluate the durability properties of SCC produced using RA from the precast industry, in order to verify the applicability of these RA in the production of high-performance concrete. In order to cover different variations in the mix proportions and the respective evaluation in mixes with different ratios of substitution of NA for RA, a total of six HPSCC mixes were produced. These mixes were selected to cover a wide range of variations from NA to RA substitution. In this sense, six replacement ratios for FRA and CRA were selected, namely: (FRA/CRA) 0/0; 25/25; 50/50; 100/100; 0/100 and 100/0%. The tests in the hardened state will be subdivided into two groups, one related to the main transport mechanisms and the other to the main degradation mechanisms. The durability study, over time, included the evaluation of open porosity (through immersion water absorption test), capillarity (through capillary water absorption test), permeability (through oxygen permeability test), diffusion (through the chloride penetration test and electrical resistivity) and carbonation (through the accelerated carbonation test). When carrying out the tests, national or international normative documents will be followed whenever possible and, when this is not possible, procedures presented in documents or reference works duly justified on a case-by-case basis will be followed.

The main final objective of this work is to provide the industry with an innovative way of appreciation the wastes resulting from the demolition of rejected precast concrete elements, through the production of HPSCC, minimizing the consumption of natural resources and, consequently, significantly decreasing its environmental impact.

2. Materials and Methods

In this section, the main properties of all materials and the mix proportions used are presented, as well as the procedures adopted in each of the tests carried out.

2.1. Materials

2.1.1. Powdery Materials

The cement used was a CEM I 52.5 R observing NP EN 197-1 [21]. Two mineral additions were also used: fly ash (FA) observing NP EN 450-1 [22] and NP EN 450-2 [23], limestone filler (LF) observing specification E466 [24] and silica fume (SF), produced according to NP EN 13263-1 [25]. Table 1 shows the main properties of cement and mineral additions.

Table 1. Chemical composition and grading of the raw materials (%).

Chemical Composition *	CEM I	FA	LF	SF
Al_2O_3	5.24	24.7	0.13	0.54
$CaCO_3$	-	-	98.35	-
CaO	62.71	2.63	-	0.43
Cl^-	0.01	<0.01	-	-
Fe_2O_3	3.17	5.4	0.03	1.15
K_2O	-	1.11	0.02	0.86
MgO	2.23	1.01	0.4	0.43

Table 1. *Cont.*

Chemical Composition *	CEM I	FA	LF	SF
Na_2O	-	0.89	-	0.29
SiO_2	19.59	54.7	0.3	93.67
SO_3	3.13	1.38	-	0.25
TiO_2	-	-	0.01	-
Insoluble Residue	1.37	-	-	-
Density (kg/m^3)	3200	2300	2720	2010
Loss of Ignition	2.94	5.1	43.8	2.54
Particle Size, in Microns *	**Passing (%)**			
1000	100	100	100	100
100	98	96	60	100
10	38	45	20	80
1	5	2	0	10
0.1	0	0	0	2
Surface Area (BET) (m^2/kg) (NP EN 196-6 [26])	325	430	456	15,000

* The chemical composition and grading of the raw materials was provided by the respective producers. CEM I: Cement type I 52.5 R; FA: Fly ash; LF: Limestone filer; SF: Silica fume.

2.1.2. Natural and Recycled Aggregates

Two limestone coarse aggregates and two siliceous sands complying with NP EN 12,620 [27], namely: gravel 1 and gravel 2, coarse sand reference 0/4 and fine sand reference 0/2.

RA from crushed concrete elements from precast industry of strength class 65 MPa: one coarse recycled aggregate (CRA) and one fine recycled aggregate (FRA). Since the RA was used in substitution of NA, its particle size distribution is the same. Table 2 shows the main properties of natural and recycled aggregates and the particle size distribution is presented in Figure 1.

Table 2. Natural and recycled aggregates properties.

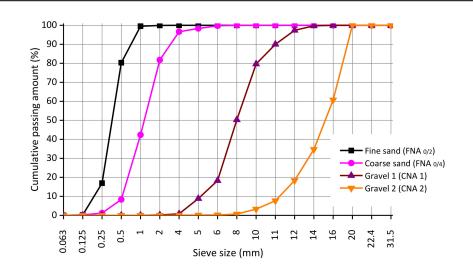| Properties	FNA		CNA		RA
	Fine Sand 0/2	Coarse Sand 0/4	Gravel 1	Gravel 2	
Density (kg/m^3)	2580	2550	2640	2690	2450
Water absorption (%)	0.7	1.1	1.6	0.8	7.5
$D_{máx}$ (mm)	2	4	11	20	20

Figure 1. Particle size distribution of the natural aggregate (NA) [28].

2.1.3. Water and Admixtures

The water used is of tap water, complying with NP EN 1008 [29] and the water-reducing admixture (Sp), in accordance with NP EN 934-1 [30] and NP EN 934-2 [31], i.e., superplasticizers with a density of 1070 kg/m^3.

2.2. Mix Proportions

For the determination of the mix proportions, the methodology proposed by Nepomuceno et al. [32–34] was followed. This methodology, in turn, is based on Japanese methods, namely the method of Okamura et al. [35] and Japan Society of Civil Engineers [36], and introduces new parameters that are better suited, for example, to the compressive strength control.

In practice, this new methodology is based, for example, on considering as variables some of the parameters previously considered constant, on the introduction of a new parameter called "mixing number" and on the consideration of a range of values for the workability parameters, instead of working with a single pair of values, among other aspects. This methodology has already been used with proven results in countless studies [37–40].

Essentially due to the size of the article, the study on the fresh-state and mechanical behavior of these HPSCC produced with recycled prefabricated aggregates is presented and evaluated in another publication, Barroqueiro et al. [41]. Thus, the present work refers exclusively the durability properties of these concrete mixes. In order to facilitate the analysis of the results presented in Section 3, Table 3 presents, in addition to the mix proportions as well as the main mix parameters, some of the basic properties of the SCC produced. With regard to the aforementioned properties, it should be noted that the results obtained in the fresh state made it possible to verify that all the mixes met the workability parameters required by the reference standard (NP EN 206-9). However, it is worth mentioning the slight loss of performance of concrete with RA when compared to the reference concrete (100% NA), essentially due to the greater water absorption of RA and also to its rougher surface compared to that of NA [41]. In terms of the mechanical properties (compressive strength and modulus of elasticity), it appears that, for the maximum replacement ratio (100% RA), they present performance losses of less than 26%. In general, it is possible to state that the differences presented are justified by the inferior quality of the RA, which is caused by the adhered mortar and which is responsible for increasing its porosity, making the ITZ (Interfacial Transition Zone) connections between the RA and the new binder weaker, as well as by the very nature of the CRA and the water it absorbs [41].

Table 3. Mix proportions and basic properties of the self-compacting concrete (SCC) produced.

Mix Proportions (kg/m^3)	100% NA	25% RA	50% RA	100% RA	100% CRA	100% FRA
CEM I 52.5 R (C)				437		
Fly Ash (FA)				145		
Limestone Filler (LF)				29		
Silica Fume (SF)				27		
Superplasticizer (S$_p$)				8		
Water (W)				193		
Sand$_{0/2}$ (FNA$_{0/2}$)	162	122	81	-	162	-
Sand$_{0/4}$ (FNA$_{0/4}$)	484	363	242	-	484	-
FRA	-	145	290	581	-	581
Gravel$_1$ (CNA$_1$)	389	292	195	-	-	389
Gravel$_2$ (CNA$_2$)	398	299	199	-	-	398
CRA	-	184	369	737	737	-
Mix Parameters						
V$_p$/V$_s$				0.800		
V$_w$/V$_P$				0.920		
S$_p$/p$_\%$				1.240		
W/C Ratio				0.442		
W/CM Ratio				0.317		
W/FM Ratio				0.303		

Table 3. *Cont.*

Mix Proportions (kg/m^3)		100% NA	25% RA	50% RA	100% RA	100% CRA	100% FRA
Basic Fresh-state Properties							
Flow Time (t$_{500}$)	[sec]	1.8	2.3	2.6	3.8	2.4	2.0
Slump-flow Diameter (SF)	[mm]	810	730	715	620	708	690
V-funnel (Tv)	[sec]	9.1	10.8	11.1	19.6	14.1	19.3
L-box (PL)		0.92	0.89	0.83	0.80	0.88	0.80
Segregated Portion (SR)	[%]	20.5	18.7	17.0	13.7	19.1	12.7
J-ring Passing Ability PJ	[mm]	5.0	7.5	9.0	10.8	8.3	1.7
Basic Mechanical Properties							
f$_{cm,c,7d}$	[MPa]	78.4	76.8	74.5	70.8	75.9	72.6
f$_{cm,c,28d}$	[MPa]	81.9	80.7	79.5	75.0	80.3	78.0
f$_{cm,c,91d}$	[MPa]	87.5	86.7	84.3	79.9	84.7	83.6
E$_{cm,28d}$	[GPa]	41.7	39.6	36.6	30.8	37.0	32.8
E$_{cm,91d}$	[GPa]	42.8	41.2	38.3	34.2	39.5	36.8

Vp/Vs = ratio, in absolute volume, between the total amount of fine materials (cement and mineral admixtures) and of fine aggregates in the mix; Vw/Vp = ratio, in absolute volume, between the total amount of water and that of fine materials; Sp/p% = percentage, in mass, of superplasticizer and fine materials in the mix; W/C = water/cement; W/CM = water/cementitious materials; W/FM = water/fine materials; fcm,c = compressive strength (15 cm × 15 cm × 15 cm cubes); Ecm = secant modulus of elasticity results (28 and 91 days).

2.3. Test Methods

2.3.1. Immersion Water Absorption Test

The immersion water absorption test was performed as per NP EN 12390-7 [42] in 100 mm cubic edge specimens. For each reference and age, three specimens were molded and tested at 28 and 91 days.

2.3.2. Capillary Water Absorption Test

The capillarity water absorption test was performed according to the E393 specification [43], at 28 and 91 days. For each reference and age, three 150 mm diameter and 100 mm high cylindrical specimens were tested. The inflow water was measured at pre-set times for the duration of the test (72 h).

2.3.3. Oxygen Permeability Test

The oxygen permeability test was performed according to the E392 specification [44], at 28 and 91 days. For each reference and age, three cylindrical specimens (50 mm height and 150 mm diameter) were tested.

2.3.4. Chloride Migration Test

The chloride migration test was carried out according to the E463 specification [45] and NT Build 492 [46], at 28 and 91 days. For each reference and age, three cylindrical specimens (50 mm height and 100 mm diameter) were tested.

2.3.5. Electrical Resistivity Test

The electrical resistivity test was performed based on the following references: Polder [47], DURAR [48] and Luping [49]. This test was carried out at 28 and 91 days. For each reference and age, three cylindrical specimens (50 mm height and 100 mm diameter) were tested.

2.3.6. Carbonation Test

The carbonation resistance test was performed according to the E391 specification [50] and "*Réunion Internationale des Laboratoires et Experts des Matériaux*" (RILEM) [51] at 7, 28, 56 and 91 days (test age begins to count at 28 days, when it is placed in the carbon dioxide chamber). For each reference

and age, to cylindrical specimens (50 mm height and 100 mm diameter) were tested. The carbonation depth was then measured using a colorimetric method (0.1% phenolphthalein).

3. Results and Discussion

The durability tests of concrete allow evaluating its behavior towards external agents (water, oxygen, carbon dioxide and chlorides). In this subchapter, the following properties were analyzed: immersion water absorption, capillarity water absorption, oxygen permeability, chloride migration, electrical resistivity and carbonation resistance.

The tests of immersion water absorption, capillarity water absorption and oxygen permeability allow evaluating the transport mechanisms inside concrete.

Tests for chloride migration, electrical resistivity and carbonation resistance penetration allow evaluating the degradation mechanisms of concrete.

3.1. Immersion Water Absorption Test

Table 4 and Figure 2 show the results obtained from the immersion water absorption test. According to them, it appears that the HPSCC with 100% FRA reached higher water absorption values, with variations in relation to the reference mix (100% NA) of 41 and 49%, at 28 and 91 days, respectively. The SCC with 100% RA is the second mix to present a worse performance in relation to the property under analysis, registered increases of 28 and 29%, at 28 and 91 days, respectively.

Table 4. Immersion water absorption results at 28 and 91 days.

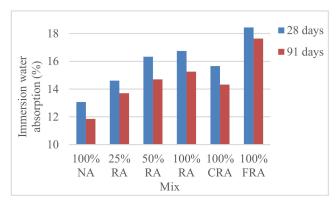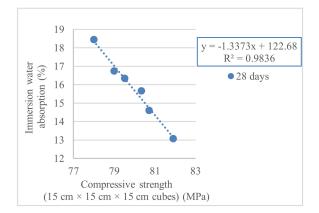| Mix	28 Days			91 Days		
	Water Absorption (%)	S.D. (%)	$\Delta_{100\% \text{ NA}}$ (%)	Water Absorption (%)	S.D. (%)	$\Delta_{100\% \text{ NA}}$ (%)
100% NA	13.07	0.16	0.0	11.85	0.14	0.0
25% RA	14.60	0.32	11.8	13.70	0.07	15.6
50% RA	16.34	0.06	25.0	14.70	0.04	24.1
100% RA	16.75	0.11	28.2	15.26	0.30	28.8
100% CRA	15.65	0.16	19.8	14.32	0.34	20.9
100% FRA	18.45	0.18	41.2	17.65	0.27	49.0

S.D. = Standard Deviation.

Figure 2. Immersion water absorption results at 28 and 91 days.

For the same property, Grdic et al. [52] find an increase of about 67% in mixes with 100% RA in relation to the reference mix. The authors justify this tendency with the higher absorption of the RA compared to the NA and the gradual increase in the W/C ratio of the mixes produced (0.41 for the SCC with 100% NA and 0.45 for the SCC with 100% RA). Similarly, Gómez-Soberón [53] states that the old mortar adhered to the RA is the main cause for the higher porosity and absorption of RA, which significantly conditions the open porosity of the SCC with RA.

Figure 3 shows the relationship between the compressive strength and its immersion water absorption. Satisfactory correlations were obtained (R^2 = 0.9836), which demonstrates the correlation between these two properties.

Figure 3. Relationship between immersion water absorption and compressive strength (15 cm × 15 cm × 15 cm cubes) results at 28 days.

3.2. Capillary Water Absorption Test

Table 5, Figures 4 and 5 and Table 6 show the results obtained from the capillary water absorption test. Analyzing Figures 4 and 5, it is possible to see that the capillary water absorption occurs more intensely in the first hours. Comparing the two figures, it is also possible to check that there is a decrease in water absorption by capillarity with age (from 28 to 91 days). This fact is explained by the decrease in average capillary pore size. The presence of fly ash causes an increase of the average pore size at younger ages; however, for older ages, there is a tendency to decrease the pore volume, reducing the possibility of water penetration [54]. Comparing the reference mix (100% NA) with the mix with 100% RA, it is possible to detect the occurrence of a 55% increase in capillary water absorption (at 28 days). These results show the same trends as Tuyan et al. [55], Modani and Mohitkar [56] and Pereira-de-Oliveira et al. [57]. Modani and Mohitkar [56] obtain an increase of 41% for mixes with 100% RA (28 days).
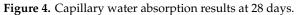
The values of the capillary coefficients of the SCC with RA were between 3.12 and 4.89×10^{-2} kg/m^2.min$^{1/2}$ at 28 days and between 1.32 and 1.13×10^{-2} kg/m^2.min$^{1/2}$ at 91 days (Table 6). Thus, increases in absorption occurred with the increase in the amount of RA. The SCC corresponding to 100% FRA replacement ratio show the worst results, with performance losses, compared to the reference SCC (100% NA), of about 57 and 17% at 28 and 91 days, respectively.

These results can be explained by the higher porosity of the RA compared to the NA due to the old mortar adhered to the first ones. Wirquin et al. [58] state that the presence of RA in concrete is the main cause for the higher volume and larger size of capillary pores.

Table 5. Capillary water absorption results at 28 and 91 days.

Mix	28 Days			91 Days		
	Capillary Absorption (kg/m^2)	S.D. (kg/m^2)	$\Delta_{100\% \text{ NA}}$ (%)	Capillary Absorption (kg/m^2)	S.D. (kg/m^2)	$\Delta_{100\% \text{ NA}}$ (%)
100% NA	0.54	0.05	0.0	0.35	0.02	0.0
25% RA	0.58	0.02	8.8	0.36	0.01	2.4
50% RA	0.67	0.02	25.3	0.38	0.02	8.4
100% RA	0.83	0.02	55.3	0.39	0.01	11.7
100% CRA	0.64	0.04	18.9	0.37	0.01	7.3
100% FRA	0.91	0.04	69.1	0.40	0.02	13.8

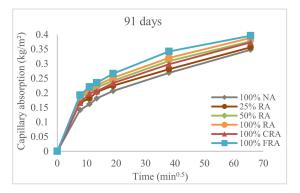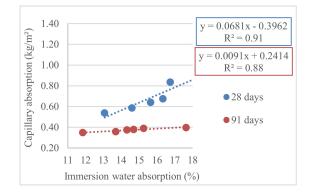**Figure 4.** Capillary water absorption results at 28 days.

Figure 5. Capillary water absorption results at 91 days.

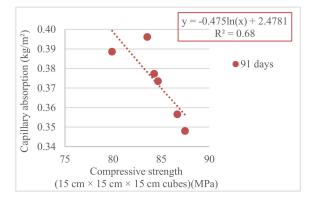**Table 6.** Capillary water absorption coefficient at 28 and 91 days.

Mix	28 Days			91 Days		
	Capillary Absorption Coefficient $(10^{-2}\text{kg}/[\text{m}^2.\text{min}^{0.5}])$	R^2	$\Delta_{100\% \text{ NA}}$ (%)	Capillary Absorption Coefficient $(10^{-2}\text{kg}/[\text{m}^2.\text{min}^{0.5}])$	R^2	$\Delta_{100\% \text{ NA}}$ (%)
100% NA	3.12	0.98	0.0	1.13	0.99	0.0
25% RA	3.52	0.98	12.8	1.17	0.97	3.5
50% RA	3.88	0.98	24.4	1.24	0.98	9.7
100% RA	3.99	0.88	27.9	1.28	0.85	13.3
100% CRA	3.75	0.98	20.2	1.23	0.97	8.8
100% FRA	4.89	0.99	56.7	1.32	0.98	16.8

Figure 6 establishes a relationship between capillary and immersion water absorption 28 and 91 days. The high correlation coefficients ($R^2 = 0.91$; $R^2 = 0.88$) show that the capillary water absorption varies linearly with the immersion water absorption. This situation is in agreement with that found by Ferreira [59].

Figure 6. Relationship between immersion water absorption and capillary water absorption results at 28 and 91 days.

Finally, in order to relate to the durability properties with the mechanical performance, the correlation between compression strength and capillary water absorption is shown in Figure 7. The correlation used was the potential non-linear since it is the one that best fits the values obtained ($R^2 = 0.68$). This situation is explained by the fact that the number of capillary pores does not grow linearly with their porosity [60].

Figure 7. Relationship between capillary water absorption and compressive strength (15 cm × 15 cm × 15 cm cubes) results at 91 days.

3.3. Oxygen Permeability Test

Table 7 and Figure 8 show the results obtained of the oxygen permeability test. It is found that the substitution of NA for RA increased the permeability to oxygen. The mix with higher oxygen permeability is the one that was produced with 100% FRA. The substitution of NA for RA increased the porosity in concrete due to the more porous nature of the first aggregates. The porous nature of RA is justified by the old mortar that is part of these aggregates [58].

Table 7. Oxygen permeability results at 28 and 91 days.

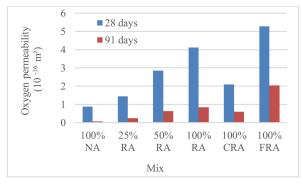| Mix	28 Days			91 Days		
	Oxygen Permeability $(10^{-16}m^2)$	S.D. $(10^{-16}m^2)$	$\Delta_{100\% \text{ NA}}$ (%)	Oxygen Permeability $(10^{-16}m^2)$	S.D. $(10^{-16}m^2)$	$\Delta_{100\% \text{ NA}}$ (%)
100% NA	0.89	0.10	0.0	0.06	0.02	0.0
25% RA	1.43	0.09	0.5	0.25	0.04	0.2
50% RA	2.84	0.17	2.0	0.63	0.02	0.6
100% RA	4.12	0.79	3.2	0.84	0.14	0.8
100% CRA	2.09	0.58	1.2	0.60	0.06	0.5
100% FRA	5.29	0.36	4.4	2.04	0.84	2.0

Figure 8. Oxygen permeability results at 28 and 91 days.

At 28 days, Zong et al. [61] obtained increases of 225% (comparing the RC with the one produced with 50% RA) and Lotfi et al. [62] achieved increases of 200% (comparing the RC with the concrete

produced with 100% RA). Similar results were obtained in the present study, i.e., there was an increase of 221% (comparing SCC with 100% NA with 50% RA) and 365% (comparing SCC with 100% NA with 100% RA).
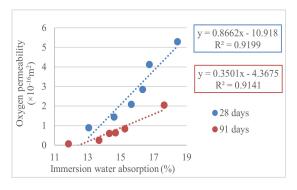
On the other hand, in identical concrete, Pereira-de-Oliveira et al. [57] were unable to obtain oxygen permeability values (even subjecting the specimen to a 3.5 bar pressure). Therefore, the authors state that, regarding this property, SCC is considered hermetic. This was confirmed by the pressure water absorption test (carried out on the same test pieces after the oxygen permeability test).

According to Table 7, and according to the RILEM [63] classification, at 28 days, mixes 100% NA and 25% RA show moderate oxygen permeability (results included in the range of 0.5 to 2.5×10^{-16} m^2), the remaining mixes have low oxygen permeability (results included in the range of 2.5–12.5×10^{-16} m^2). At 91 days, the 100% NA and 25% RA mixes have good resistance to oxygen penetration and the remaining mixes have moderate resistance to oxygen penetration.
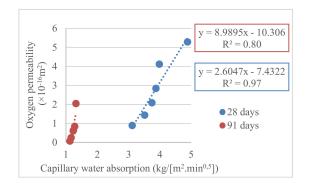
The decrease in oxygen permeability with age can be explained by the presence of fly ash in concrete that only begins to react at older ages [64]. Thus, in the early ages, the effect of RA on concrete is relevant and, with increasing age, this effect is replaced by the effect of fly ash. The pozzolanic reaction of fly ash with cement is responsible for filling the concrete pores, making it difficult for oxygen to penetrate. This fact is also confirmed by the capillarity water absorption test.

The penetration of oxygen into concrete is strongly related to the other transport mechanisms, namely the absorption of water by immersion and capillarity.

Thus, by relating oxygen penetration to water penetration by immersion, correlation coefficients of 0.93 and 0.91 were obtained at 28 and 91 days, respectively (Figure 9). Relating oxygen penetration to water penetration by capillarity, correlation coefficients of 0.97 and 0.80 were obtained at 28 and 91 days, respectively (Figure 10).

Figure 9. Relationship between oxygen permeability and immersion water absorption results at 28 and 91 days.

Figure 10. Relationship between oxygen permeability and capillary water absorption results at 28 and 91 days.

3.4. Chloride Migration Test

Table 8 and Figure 11 show the results obtained from the chloride migration test. Figure 11 shows that the presence of RA increases the penetration of chloride ions. At 28 days, the mix with 100% RA shows a 41% increase in chloride migration coefficient compared to the 100% NA SCC. Modani and Mohitkar [58] obtained results in the same order of magnitude: 62%. The increase observed is explained by the higher porosity of the RA compared to the NA, due to the old mortar that is part of the RA [58]. Another factor that may explain this trend is the size of the cracks in the RA. Xiao et al. [65] concluded that the crack width existing in the old adhered mortar is correlated with the chloride diffusion coefficient, with greater diffusion for larger crack widths. The higher coefficient is found in the mix with 100% FRA, with an increase of 49% and 58% at 28 and 91 days (Table 8). This is explained by the poorer quality of the SCC paste (due to the substitution of FNA with FRA), since ion transport is preferably done in that area.

Table 8. Chloride migration results at 28 and 91 days.

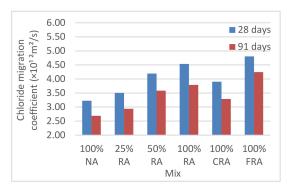| Mix	28 Days			91 Days		
	Chloride Migration Coefficient ($\times 10^{-12}$ m^2/s)	S.D. ($\times 10^{-12}$ m^2/s)	$\Delta_{100\% \text{ NA}}$ (%)	Chloride Migration Coefficient ($\times 10^{-12}$ m^2/s)	S.D. ($\times 10^{-12}$ m^2/s)	$\Delta_{100\% \text{ NA}}$ (%)
100% NA	3.2	0.5	0.0	2.7	0.1	0.0
25% RA	3.5	0.8	8.7	2.9	0.6	9.2
50% RA	4.2	0.5	30.1	3.6	0.5	33.2
100% RA	4.5	0.5	40.8	3.8	0.2	41.0
100% CRA	3.9	0.4	21.1	3.3	0.2	22.2
100% FRA	4.8	0.7	49.2	4.2	0.4	58.0

Figure 11. Chloride migration results at 28 and 91 days.

Comparing the chloride migration coefficient with other properties also responsible for the transport mechanisms inside concrete enables establishing correlations. Thus, through Figures 12 and 13, it is possible to observe the existence of a correlation between the chloride diffusion coefficient and immersion water absorption ($R^2 = 0.61$) and between chloride diffusion coefficient and water absorption by capillarity ($R^2 = 0.80$).
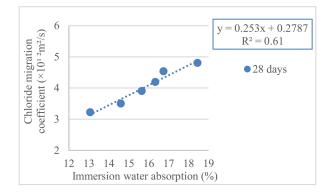

Figure 12. Relationship between chloride migration and immersion water absorption results at 28 days.
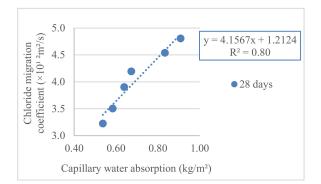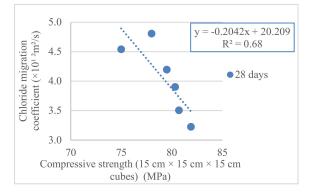
Figure 13. Relationship between chloride migration and capillary water absorption results at 28 days.

In order to relate the property under analysis to the mechanical strength of concrete, Figure 14 is presented, which relates the compressive strength with the chloride diffusion coefficient.

Figure 14. Relationship between chloride migration and compressive strength (15 cm × 15 cm × 15 cm cubes) results at 28 days.

3.5. Electrical Resistivity Test

Table 9 and Figure 15 show the results from the electrical resistivity test. It turns out that electrical resistivity decreases with the substitution of NA for RA. For the mix with 100% RA, reductions of 27% and 30% occur at 28 and 91 days of age, respectively. Surya et al. [66] and Andreu and Miren [67] obtained reductions of 36 and 33%, respectively (comparing the RC with the concrete in which only RA were used). This is justified by the higher porosity of the RA compared to the NA, due to the old mortar that is part of the RA.

Table 9. Electrical resistivity results at 28 and 91 days.

Mix	28 Days			91 Days		
	Electrical Resistivity (Ω.m)	S.D. (Ω.m)	$\Delta_{100\% \text{ NA}}$ (%)	Electrical Resistivity (Ω.m)	S.D. (Ω.m)	$\Delta_{100\% \text{ NA}}$ (%)
100% NA	247.0	11.4	0.0	556.2	18.0	0.0
25% RA	238.5	9.9	−3.4	530.1	31.9	−4.7
50% RA	185.4	10.3	−24.9	407.9	14.4	−26.7
100% RA	180.2	6.0	−27.0	391.4	34.3	−29.6
100% CRA	198.6	1.3	−19.6	441.0	22.8	−20.7
100% FRA	166.7	22.8	−32.5	320.2	11.1	−42.4

Figure 16 establishes a relationship between electrical resistivity and the chloride diffusion coefficient. The determination coefficients ($R^2 = 0.88$; $R^2 = 0.99$) show that these two properties are strongly correlated. Regarding these two parameters that can be used for the evaluation of the diffusion mechanism in concrete, it appears that the electrical resistivity is inversely proportional to the diffusion

process of chloride ions (as noted by Santos et al. [40]). The electrical resistivity evaluates the ability of an element to resist the passage of a current, and in this test the migration of all ions is evaluated. On the other hand, the diffusion coefficient assesses the element's resistance to the penetration of chloride ions.
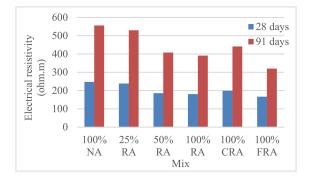

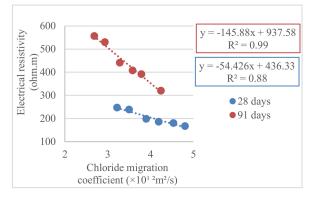**Figure 15.** Electrical resistivity results at 28 and 91 days.

Figure 16. Relationship between chloride migration and electrical resistivity results at 28 and 91 days.

In practice, the electrical resistivity, unlike the chloride diffusion coefficient, depends on all the ions in the paste, especially hydroxides. Thus, electrical resistivity is strongly influenced by the presence, for example, of pozzolanic additions, such as fly ash [48].

3.6. Carbonation Test

Table 10 and Figure 17 show the results of the carbonation test. It is found that, in the first ages (7 and 28 days), the effect of CO_2 is non-existent. The CO_2 only starts to penetrate after 56 days, although with penetration depths below 2 mm (considerably low values). The reduced depths of CO_2 penetration are justified by the low w/c ratio (0.44). Siddique [68] presents carbonation depths below 2 mm, for 90 days of exposure to CO_2, in SCC mixes with a w/c ratio of 0.44. Bogas [37] refers to negligible carbonation depth in concrete with a w/c ratio below 0.35. The author states that, regardless of the type of concrete analyzed, it only obtained carbonation in the surface layer, in thicknesses between 1 and 2 mm, after one year of exposure in the carbonation chamber.

The absence of depth of carbonation at early ages is also explained by the fact that these mixes are of HPSCC. This implies a strengthening of the interface transition zones, contributing to a better performance of concrete. In this context, silica fume is one of the most relevant components. Silica fume is responsible for decreasing the porosity and permeability of concrete, a consequence of its small size and ability to create a large number of nucleation sites for precipitation of hydration products. Consequently, silica contributes to increasing the durability of HPSCC [69,70].

Table 10. Carbonation test results at 7, 56, 28 and 91 days.

Mix	7 Days			28 Days			56 Days			91 Days		
	Carbonation Depth (mm)	S:D: (mm)	$\Delta_{100\% NA (\%)}$	Carbonation Depth (mm)	S:D: (mm)	$\Delta_{100\% NA (\%)}$	Carbonation Depth (mm)	S:D: (mm)	$\Delta_{100\% NA (\%)}$	Carbonation Depth (mm)	S:D: (mm)	$\Delta_{100\% NA (\%)}$
100% NA	0	0	0	0	0	0.0	0.4	0.1	0.0	0.8	0.2	0.0
25% RA	0	0	0	0	0	0.0	0.8	0.2	83.4	1.2	0.3	50.7
50% RA	0	0	0	0	0	0.0	1.1	0.6	155.8	1.6	0.4	93.4
100% RA	0	0	0	0	0	0.0	1.3	0.4	206.8	2.1	0.4	162.9
100% CRA	0	0	0	0	0	0.0	1.0	0.1	121.6	1.5	0.4	85.0
100% FRA	0	0	0	0	0	0.0	1.9	0.9	347.4	2.2	0.2	172.2

Figure 17. Carbonation test results at 7, 56, 28 and 91 days.

The carbonation depth values tend to increase as the ratio of substitution of NA for RA increases. For SCC with 100% RA, the carbonation depth increased 207% and 163% at 56 and 91 days, respectively. This situation is in line with what was expected, since water absorption (by immersion and capillarity) showed a similar trend.

A justification for the greater depth of carbonation in SCCs with RA is related to the higher porosity of these concrete mixes, where it is found that the total volume and the average pore diameter increase with the incorporation of RA [71].

Carbonation can be characterized by its coefficient, by varying the depth of carbonation over time, with expression (1):
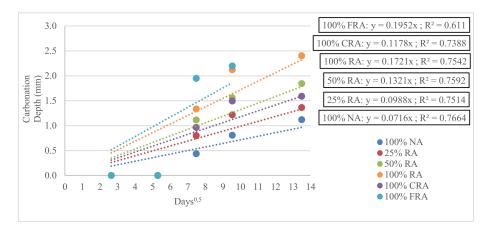
$$x = kt^{\frac{1}{n}} \ (\text{with } n = 2) \tag{1}$$

x = carbonation depth;
k = carbonation coefficient;
t = time.

With the analysis of Figure 18 as well as of Table 11, it is found that the variation in the carbonation depth over time is adequately characterized by Equation (1), presenting reasonable correlation coefficients, always greater than 0.7, with the exception of the 100% FRA mix. However, according to what was reported by Neville [72] and Bertolini et al. [73], among others, the aforementioned expression involving the square root of time is not the most suitable for non-stationary exposure conditions, i.e., in situations of natural exposure, in which the concrete is subject to variations in humidity, temperature and levels of CO_2 concentrations significantly lower than those of the accelerated test. Bertolini et al. [73] state that, for concrete in conditions of natural exposure, the reduction of the carbonation process over time is more accentuated than that described by the parabolic expression (1) and that, in these cases, "n" can tend to values slightly more than 2. As observed in the present study, Bertolini et al. [73] state that, in concrete with higher compactness, the carbonation process tends to be negligible.

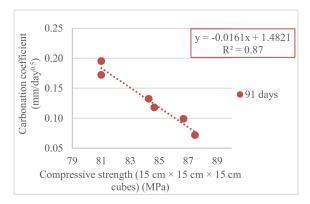**Figure 18.** Depths of carbonation as function of $\sqrt{t}$ for all mixes.

Table 11. Carbonation coefficients for all mixes.

Mix	Carbonation Coefficient (mm/day$^{0.5}$)	R^2	$\Delta_{100\% \text{ NA}}$ (%)
100% NA	0.0716	0.7664	0.0
25% RA	0.0988	0.7514	38.0
50% RA	0.1321	0.7592	84.5
100% RA	0.1721	0.7542	140.4
100% CRA	0.1178	0.7388	64.5
100% FRA	0.1952	0.6110	172.6

As seen in the other properties, the greatest variation was registered for the replacement ratio of 100% AFR, in relation to the 100% NA mix (172.6%). However, it should be noted that all the mixes have very low and almost a negligible carbonation coefficient value if an exposure time in an accelerated carbonation chamber of 91 days is taken into account.
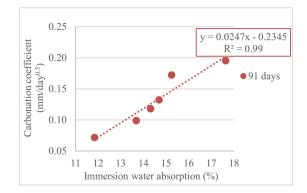
In the particular case of these mixes (see Table 3), it is also possible to highlight the influence of fly ash specifically on the action of the carbonation degradation mechanism. Thus, two main consequences (one negative and the other positive) in its use in substitution of cement in the manufacture of concrete are highlighted. The negative consequence is associated with the lower content of calcium hydroxide ($Ca(OH)_2$) resulting from the use of fly ash, which causes a decrease in the capacity of CO_2 fixation by the paste, so inevitably lower concentrations of CO_2 to carbonate the concrete are needed. The positive consequence of the use of fly ash is due to the improvement of the microstructure of the paste matrix, which, as confirmed in the present work, is reflected in a network of smaller capillary pores when compared to mixes without fly ash.

Given the high value of the correlation coefficient ($R^2 = 0.87$), it is possible to see a linear relationship between the carbonation depth and the compressive strength in cubes (Figure 19).
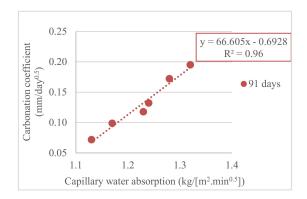

Figure 19. Relationship between the carbonation coefficients and compressive strength (15 cm × 15 cm × 15 cm cubes) results at 91 days.

It is also possible to see a linear relationship between carbonation and water absorption properties by immersion (Figure 20) and by capillarity (Figure 21), given the values of the correlation coefficient ($R^2 = 0.99$ and $R^2 = 0.96$, respectively).

Figure 20. Relationship between the carbonation coefficients and immersion water absorption results at 91 days.

Figure 21. Relationship between the carbonation coefficients and capillary water absorption results at 91 days.

4. Concluding Remarks

This work intended to analyze the experimental results obtained during the production of HPSCC with RA. In this sense, six types of SCC were produced incorporating different amounts of RA. Six replacement ratios for FRA and CRA were considered: (FRA/CRA) 0/0; 25/25; 50/50; 100/100; 0/100 and 100/0%.

In order to facilitate the global analysis of the results obtained, in Table 12, a summary was presented, where the comparisons were made, basically, between reference HPSCC (with 100% NA) and all the other mixes, and the maximum increase or decrease are presented.

Table 12. Tests results summary at 28 days for all mixes.

Durability Properties	Mix and Respective Increase/Decrease Relative to the Reference 100% NA (%)				
	25% RA	**50% RA**	**100% RA**	**100% CRA**	**100% FRA**
Immersion Water Absorption	[a] 12	25	28	20	[b] 41
Capillary Water Absorption	[a] 9	25	55	19	[b] 69
Oxygen Permeability	[a] 63	221	365	136	[b] 497
Chloride Migration	[a] 9	30	41	21	[b] 49
Electrical Resistivity	[a] −3	−25	−27	−20	[b] −33
Carbonation Test (91 days)	[a] 51	93	163	85	[b] 172

[a] Better result [b] Worse result.

The results in Table 12 show that the different mixes incorporating RA show consistent variations. It appears that the mix with 25% RA presents the best performance, with losses below 12% (except in oxygen permeability, in which it presents a loss of 63%, and in carbonation, in which it presents a loss of 51%).

For all properties under analysis, the mixes with 50% RA and 100% CRA show a similar performance in terms of durability. Additionally, the first one tends to have worse results than the second.

In terms of durability, the HPSCC with 100% FRA performed less favorably than the one with 100% RA. Comparing the two mixes (100% RA and 100% FRA), it appears that both have 100% FRA replacing FNA, only differing in the nature of the CA (presenting 100% CRA and 100% CNA, respectively). Consequently, the differences recorded may be justified by the nature of the coarse aggregates and the water they absorb.

The high-water absorption of RA causes the need to correct the amount of mixing water (taking into account the values that will be absorbed). This correction of mixing water can cause the retention of significant amounts of water (by the RA) during the initial moments of the mixing process. That water will not contribute to the workability of concrete or obviously to the hydration process of cement (at least at early ages), but it will later be released under these conditions and may significantly contribute to the later reaction of fly ash with calcium oxide or with calcium hydroxide (products resulting from hydration of the cement).

The aforementioned reaction of fly ash with cement hydration products, when aided by the additional "supply" of water, will form more favorably (when compared to the SCC of 100% FRA, i.e., without CRA) products similar to those produced by the reaction of cement with water (hydrated calcium silicates). Therefore, it is considered that the aforementioned additional water supply (essential for the reaction of fly ash with calcium oxide or calcium hydroxide) will contribute decisively to the improvement of the microstructure of the concrete in question, consequently causing an increased compactness, with direct implications in improving its durability properties (both in transport and degradation mechanisms).

Regarding oxygen permeability, water absorption by immersion and capillarity, there is a decrease in performance in these properties due to the incorporation of RA in concrete. The presence of old mortar adhered to RA is responsible for the higher porosity of concrete.

In these three phenomena, there is a decrease in the penetration of oxygen and water with age. This fact is explained by the reduction of the capillary pores. The presence of fly ash causes an increase of the average pore size at younger ages; however, for older ages, there is a tendency for the pore volume to decrease, causing the penetration rate to decrease.

The increase in the substitution of NA for RA in the SCC increased the penetration of chloride ions (increased from 9% to 49%, at 28 days). This fact is explained by the degradation of the quality of the SCC paste (due to the substitution of sand by FRA), since the transport of ions is preferably done in that area.

When analyzing the transport of all types of ions in the SCC (through the electrical resistivity test), it appeared that it increased with the replacement of NA with RA, which is in accordance with the ion penetration test chloride. Increased from 3% to 33% occur at 28 days.

At early ages, the carbonation of concrete was imperceptible and only began to be visible after 56 days of exposure to CO_2 in an accelerated carbonation chamber, although with very low values (less than 2 mm). This fact was explained by the low w/c ratio used in the mixes (0.44). The carbonation depth values tended to increase with the ratio of substitution of NA for RA. This situation is in line with expectations, since water absorption (by immersion and capillarity) had a similar trend.

References

1. World Business Council for Sustainable Development (WBCSD); International Energy Agency (IEA). *Technology Roadmap, Low-Carbon Transition in the Cement Industry*; IEA: Paris, France, 2018; p. 66.

2. Department of Trade and Industry (DTI). *Energy White Paper: Our Energy Future Creating a Low Carbon Economy*; DTI: London, UK, 2003; p. 138.

3. Zhang, T.; Gao, P.; Gao, P.; Wei, J.; Yu, Q. Effectiveness of novel and traditional methods to incorporate industrial wastes in cementitious materials: An overview. *Resour. Conserv. Recycl.* **2013**, *74*, 134–143. [CrossRef]

4. Jani, Y.; Hogland, W. Waste glass in the production of cement and concrete: A review. *J. Environ. Chem. Eng.* **2012**, *2*, 1767–1775. [CrossRef]

5. Silva, P.R.; de Brito, J. Fresh-State Properties of Self-Compacting Mortar and Concrete with Combined Use of Limestone Filler and Fly Ash. *Mat. Res. Ib Am. J. Mat.* **2015**, *18*, 1097–1108. [CrossRef]

6. British Precast Concrete Association (BPCA). *Precast Sustainability Strategy and Charter*; BPCA: Leicester, UK, 2013.

7. European Commission (EC). Directive 2008/98/EC of the European Parliament and of the Council of 19 November 2008 on waste. *O. J. Euro. Un.* **2008**, *312*, 11–22.

8. Ozbakkaloglu, T.; Gholampour, A.; Xie, T. Mechanical and durability properties of recycled aggregate concrete: Effect of recycled aggregate properties and content. *J. Mat. Civ. Eng.* **2018**, *30*. [CrossRef]

9. Dimitriou, G.; Savva, P.; Petrou, M.F. Enhancing mechanical and durability properties of recycled aggregate concrete. *Constr. Build. Mater.* **2018**, *158*, 228–235. [CrossRef]

10. Alexandridou, C.; Angelopoulos, G.N.; Coutelieris, F.A. Mechanical and durability performance of concrete produced with recycled aggregates from Greek construction and demolition waste plants. *J. Clean. Prod.* **2018**, *176*, 745–757. [CrossRef]

11. Poon, C.S.; Shui, Z.H.; Lam, L. Effect of microstructure of ITZ on compressive strength of concrete prepared with recycled aggregates. *Constr. Build. Mater.* **2004**, *18*, 461–468. [CrossRef]

12. Poon, C.S.; Shui, Z.H.; Lam, L.; Fok, H.; Kou, S.C. Influence of moisture states of natural and recycled aggregates on the slump and compressive strength of concrete. *Cem. Concr. Res.* **2004**, *34*, 31–36. [CrossRef]

13. Tam, V.W.Y.; Gao, X.F.; Tam, C.M. Microstructural analysis of recycled aggregate concrete produced from two-stage mixing approach. *Cem. Concr. Res.* **2005**, *35*, 1195–1203. [CrossRef]

14. Evangelista, L.; de Brito, J. Mechanical behaviour of concrete made with fine recycled concrete aggregates. *Cem. Concr. Compos.* **2007**, *29*, 397–401. [CrossRef]

15. Thomas, C.; Cimentada, A.; Polanco, J.A.; Setién, J.; Méndez, D.; Rico, J. Influence of recycled aggregates containing sulphur on properties of recycled aggregate mortar and concrete. *Comp. Part B Eng.* **2013**, *45*, 474–485. [CrossRef]

16. Soares, D.; de Brito, J.; Ferreira, J.; Pacheco, J. Use of coarse recycled aggregates from precast concrete rejects: Mechanical and durability performance. *Constr. Build. Mater.* **2014**, *71*, 263–272. [CrossRef]

17. Thomas, C.; Setién, J.; Polanco, J.A. Structural recycled aggregate concrete made with precast wastes. *Constr. Build. Mater.* **2016**, *114*, 536–546. [CrossRef]

18. Xiao, J.; Jiang, X.; Huang, Y.; Gao, G. Test on the mechanical behavior of semiprecast recycled concrete elements, Tumu Gongcheng Xuebao/China. *Civ. Eng. J.* **2013**, *46*, 99–104.

19. Chen, W.; Jin, R.; Xu, Y.; Wanatowski, D.; Li, B.; Yan, L.; Pan, Z. Adopting recycled aggregates as sustainable construction materials: A review of the scientific literature. *Constr. Build. Mater.* **2019**, *218*, 483–496. [CrossRef]

20. Fiol, F.; Thomas, C.; Muñoz, C.; Ortega-López, V.; Manso, J.M. The influence of recycled aggregates from precast elements on the mechanical properties of structural self-compacting concrete. *Constr. Build. Mater.* **2018**, *182*, 309–323. [CrossRef]

21. Instituto Português da Qualidade (IPQ). *Cement, Part 1: Composition, Specifications and Conformity Criteria for Common Cements*; IPQ: Lisbon, Portugal, 2008; p. 8.

22. Instituto Português da Qualidade (IPQ). *NP EN 450-1, A1, Fly Ash for Concrete, Part 1: Definition, Specifications and Conformity Criteria*; IPQ: Lisbon, Portugal, 2008; p. 35.

23. Instituto Português da Qualidade (IPQ). *NP EN 450-2, 2006, Fly Ash for Concrete, Part 2: Conformity Evaluation*; IPQ: Lisbon, Portugal, 2006; p. 29.

24. LNEC E 466. *Limestone Fillers for Hydraulic Binders*; National Laboratory for Civil Engineering: Lisbon, Portugal, 2005; p. 2. (In Portuguese)

25. Instituto Português da Qualidade (IPQ). *25 Silica Fume for Concrete—Part 1: Definitions, Requirements and Conformity Criteria (Includes Amendment A1:2009)*; IPQ: Lisbon, Portugal, 2005.

26. Instituto Português da Qualidade (IPQ). *NP EN 196-6, Methods of Testing Cement—Part 6: Determination of Fineness*; IPQ: Lisbon, Portugal, 2010; p. 20.

27. Instituto Português da Qualidade (IPQ). *NP EN 12620, Aggregates for Concrete*; IPQ: Lisbon, Portugal, 2010; p. 61.

28. Santos, S.; Silva, P.R.; de Brito, J. Mechanical performance evaluation of self-compacting concrete with fine and coarse recycled aggregates from precast industry. *Materials* **2017**, *10*, 904. [CrossRef]

29. Instituto Português da Qualidade (IPQ). *Mixing Water for Concrete, Specification for Sampling, Testing and Assessing the Suitability of Water, Including Water Recovered from Processes in the Concrete Industry, as Mixing Water for Concrete*; IPQ: Lisbon, Portugal, 2003; p. 22.

30. Instituto Português da Qualidade (IPQ). *Admixtures for Concrete, Mortar and Grout, Part 1: Common Requirements*; IPQ: Lisbon, Portugal, 2008; p. 13.

31. Instituto Português da Qualidade (IPQ). *Admixtures for Concrete, Mortar and Grout, Part 2: Concrete Admixtures, Definitions, Requirements, Conformity, Marking and Labelling*; IPQ: Lisbon, Portugal, 2009; p. 28.

32. Nepomuceno, M.; Oliveira, L. Parameters for self-compacting concrete mortar phase. *ACI Mat. J.* **2008**, *253*, 323–340.

33. Nepomuceno, M.; Oliveira, L.; Lopes, S.M.R. Methodology for mix design of the mortar phase of self-compacting concrete using different mineral additions in binary blends of powders. *Constr. Build. Mater.* **2012**, *26*, 317–326. [CrossRef]

34. Silva, P.; de Brito, J.; Costa, J. Viability of two new mix design methodologies for SCC. *ACI Mat. J.* **2011**, *108*, 579–588.

35. Okamura, H.; Ozawa, K.; Ouchi, M. Self-compacting concrete. *Struct. Conc. J.* **2000**, *1*, 3–17. [CrossRef]

36. JSCE (Japan Society of Civil Engineers). Recommendation for construction of self-compacting concrete. In Proceedings of the International Workshop on Self-compacting Concrete, Kochi, Japan, 23–26 August 1998; pp. 417–437.

37. Bogas, J.; Gomes, A.; Pereira, M. Self-compacting lightweight concrete produced with expanded clay aggregate. *Constr. Build. Mater.* **2012**, *35*, 1013–1022. [CrossRef]

38. Rao, S.V.; de Brito, J.; Silva, P. Experimental study of the mechanical properties and durability of self-compacting mortars with nano materials (SiO_2 and TiO_2). *Constr. Build. Mater.* **2015**, *96*, 508–517. [CrossRef]

39. Silva, P.; de Brito, J. Experimental study of mechanical properties and shrinkage in self-compacting concrete with binary and ternary mixtures of fly ash and limestone filler. *Eur. J. Environ. Civ. Eng.* **2017**, *21*, 430–453. [CrossRef]

40. Santos, S.; Silva, P.; Brito, J. Durability evaluation of self-compacting concrete with recycled aggregates from the precast industry. *Mag. Concr. Res.* **2019**, *71*, 1265–1282. [CrossRef]

41. Barroqueiro, T.; Silva, P.; Brito, J. Fresh-state and mechanical properties of high-performance self-compacting concrete with recycled aggregates from the precast industry. *Materials* **2019**, *2*, 3565. [CrossRef]

42. Instituto Português da Qualidade (IPQ). *Testing Hardened Concrete, Part 7: Density of Hardened Concrete*; IPQ: Lisbon, Portugal, 2009; p. 14.

43. LNEC E393. *Concrete. Determination of the Absorption of Water through Capillarity*; National Laboratory for Civil Engineering: Lisbon, Portugal, 1993; p. 2.

44. LNEC E392. *Concrete. Determination of the Oxygen Permeability*; National Laboratory for Civil Engineering: Lisbon, Portugal, 1993.

45. LNEC E463. *Concrete. Determination of Diffusion Coefficient of Chlorides from Non-Steady-State Migration Test*; National Laboratory for Civil Engineering: Lisbon, Portugal, 2004; p. 8.

46.	Nordtest NT Build 492. *Concrete, Mortar and Cement-Based Repair Materials, Chloride Migration Coefficient from Non-Steadystate Migration Experiments*; Nordtest: Espoo, Finland, 1999.

47.	Polder, R. Test methods for on-site measurement of resistivity of concrete, Rilem TC 154-EMC: Electrochemical techniques for measuring metallic corrosion. *Mater. Struct.* **2000**, *15*, 125–131.

48.	Ibero-American Program Science and Technology for Development. *DURAR, Thematic Network XV.B Durability of Rebars, Manual for Inspecting, Evaluating and Diagnosing Corrosion in Reinforced Concrete Structures. CYTED, Ibero-American Program Science and Technology for Development, Subprogram XV, Corrosion/Environmental Impact on Materials, Maracaibo, Venezuela*; Ibero-American Program Science and Technology for Development: Maracaibo, Venezuela, 2000; ISBN 980-296-541-3.

49.	Luping, T. Guidelines for Practical Use of Methods for Testing the Resistance of Concrete to Chloride Ingress, EU-Project Chlortest (EU Funded Research Project under 5FP GROWTH Programme). Swedish National Testing and Research Institute: Boras, Sweden, 2005.

50.	LNEC E391. *Concrete, Determination of Carbonation Resistance*; National Laboratory for Civil Engineering: Lisbon, Portugal, 1993; p. 2.

51.	RILEM (Réunion Internationale des Laboratoires et Experts des Matériaux). CPC-18: Measurement of hardened concrete carbonation depth. *Mater. Struct.* **1998**, *21*, 453–455.

52.	Grdic, Z.J.; Toplicic-Curcic, G.A.; Despotovic, I.M.; Ristic, N.S. Properties of self-compacting concrete prepared with coarse recycled concrete aggregate. *Constr. Build. Mater.* **2010**, *24*, 1129–1133. [CrossRef]

53.	Gómez-Soberón, J. Porosity of recycled concrete with substitution of recycled concrete aggregate: An experimental study. *Cem. Concr. Res.* **2002**, *32*, 1301–1311.

54.	RILEM (Réunion Internationale des Laboratoires et Experts des Matériaux). *Report 7, Fly Ash in Concrete, Properties and Performance, Report of Technical Committee 67-FAB use of Fly Ash in Building*; Wesche, K., Ed.; RILEM Publications: Bagneux, France, 1991; p. 284. ISBN 0-203-62641-9.

55.	Tuyan, M.; Mardani-Aghabaglou, A.; Ramyar, K. Freeze–thaw resistance, mechanical and transport properties of self-consolidating concrete incorporating coarse recycled concrete aggregate. *Mater. Des.* **2014**, *53*, 983–991. [CrossRef]

56.	Modani, P.O.; Mohitkar, V.M. Self-compacting concrete with recycled aggregate: A solution for sustainable development. *Int. J. Civ. Struct. Eng.* **2014**, *4*, 430–440.

57.	Pereira-de-Oliveira, L.; Nepomuceno, M.C.S.; Castro-Gomes, J.P.; Vila, M.F.C. Permeability properties of self-compacting concrete with coarse recycled aggregates. *Constr. Build. Mater.* **2014**, *51*, 113–120. [CrossRef]

58.	Wirquin, E.; Hadjieva-Zaharieva, R.; Buyle-Bodin, F. Use of water absorption by concrete as a criterion of the durability of concrete—Application to recycled aggregate concrete. *Mater. Struct.* **2000**, *33*, 403–408. [CrossRef]

59.	Ferreira, R. Probability-Based Durability Analysis of Concrete Structures in Marine Environment. Ph.D. Thesis, Civil Engineering, University of Minho School of Engineering Department of Civil Engineering, Guimarães, Portugal, 2004; p. 339.

60.	Siddique, R.; Cachim, P. *Waste and Supplementary Cementitious Materials in Concrete, Characterisation, Properties and Applications*, 1st ed.; Woodhead Publishing Series in Civil and Structural Engineering; Woodhead Publishing: Cambridge, UK, 2018; p. 640.

61.	Zong, L.; Fei, Z.; Zhang, S. Permeability of recycled aggregate concrete containing fly ash and clay brick waste. *J. Clean. Prod.* **2014**, *70*, 175–182. [CrossRef]

62.	Lotfi, S.; Eggimann, M.; Wagner, E.; Mróz, R.; Deja, J. Performance of recycled aggregate concrete based on a new concrete recycling technology. *Constr. Build. Mater.* **2015**, *95*, 243–256. [CrossRef]

63.	RILEM (Réunion Internationale des Laboratoires et Experts des Matériaux). Recommendation of TC 116-PCD—Tests for gas permeability of concrete. *Mater. Struct.* **1999**, *32*, 1359–5997.

64.	Camões, A. Betões de Elevado Desempenho com Incorporação de Cinzas Volantes. Ph.D. Thesis, University of Minho, Guimarães, Portugal, 2002. (In Portuguese).

65.	Xiao, J.; Li, J.; Zhang, C. Mechanical properties of recycled aggregate concrete under uniaxial loading. *Cem. Concr. Res.* **2005**, *35*, 1187–1194. [CrossRef]

66.	Surya, M.; Rao, K.; Lakshmy, P. Recycled aggregate concrete for transportation infrastructure. *Procedia Soc. Behav. Sci.* **2013**, *104*, 1158–1167. [CrossRef]

67.	Andreu, G.; Miren, E. Experimental analysis of properties of high performance recycled aggregate concrete. *Constr. Build. Mater.* **2014**, *52*, 227–235. [CrossRef]

68. Siddique, R. Properties of self-compacting concrete containing class F fly ash. *Mater. Des.* **2011**, *32*, 1501–1507. [CrossRef]
69. Parande, A. *Role of Ingredients for High Strength and High Performance Concrete—A Review*; CSIR-Central Electrochemical Research Institute Karaikudi: Tamil Nadu, India, 2013; p. 12.
70. Ramezanianpour, A.; Rezaei, H.; Savoj, H. *Influence of Silica Fume on Chloride Diffusion and Corrosion Resistance of Concrete—A Review*; Department of Civil and Environmental Engineering, Amir Kabir University of Technology: Tehran, Iran, 2014; p. 21.
71. Kou, S.; Poon, C. Compressive strength, pore size distribution and chloride-ion penetration of recycled aggregate concrete incorporating class-F fly ash, J.W. *Uni. Tech. Mater. Sci. Ed.* **2006**, *21*, 130–136.
72. Neville, A.M. *Properties of Concrete*, 4th ed.; Pearson: London, UK, 1995; p. 844.
73. Bertolini, L.; Elesener, B.; Pedeferri, P.; Polder, R. *Corrosion of Steel in Concrete, Prevention, Diagnosis, Repair*; WILEY-VCH Verlag GmbH & Co. KGaA: Weinheim, Germany, 2004; p. 392.